Research Article

Selective Inhibition of Intracellular Kv1.3 Potassium Channels by Lentivirus-Mediated Expression of Agitoxin

Jay Yang[1*], Takeshi Suzuki[1,2], Maya Mikami[3]

[1]Department of Anesthesiology, University of Wisconsin, SMPH Madison, WI, USA

[2]Department of Anesthesiology, Tokai University School of Medicine, Kanagawa, Japan

[3]Columbia University College of Physicians & Surgeons, New York, NY, USA

[*]Corresponding Author

Jay Yang, Department of Anesthesiology University of Wisconsin SMPH 1111 Highland Avenue, WIMR 8451 Madison, WI 53705, USA, Tel: 608-265-6710; E-mail: Jyang75@wisc.edu

Received: 26 August 2019; **Accepted:** 09 September 2019; **Published:** 16 September 2019

Citation: Jay Yang, Takeshi Suzuki, Maya Mikami. Selective Inhibition of Intracellular Kv1.3 Potassium Channels by Lentivirus-Mediated Expression of Agitoxin. Journal of Biotechnology and Biomedicine 2 (2019): 084-095.

Abstract

Non-plasma membrane Kv1.3 voltage-gated potassium channels, particularly those localized to the inner mitochondrial membrane, is pro-survival in that inhibition of these channels enhances apoptosis of cancer cells. Paradoxically, cells that lack Kv1.3 show resistance to cytotoxic agents suggesting a pro-death role of the same channels. Currently reported genetic and pharmacological reagents block both plasma membrane and intracellular Kv1.3 and lack absolute selectivity for intracellular Kv1.3. We designed a lentivirus for intracellular expression of the Kv1.3-selective peptide toxin agitoxin and created a Jurkat lymphocyte cell line that constitutively expressed intracellular agitoxin to selectively inhibit intracellular Kv1.3. Agitoxin-expressing Jurkat cells demonstrated relative resistance to cytokine-induced apoptosis, whereas direct extracellular application of agitoxin, or control cells expressing EGFP alone, failed to demonstrate this cyto- protection. We concluded that the intracellular Kv1.3 served a pro-death role, and a selective inhibition of this target reduced lymphocyte apoptosis by cytokine stimulation as reported previously for Kv1.3-null cells.

Keywords: Cytokine; Lentivirus; Jurkat; CTLL-2; Agitoxin; Kv1.3

1. Introduction

Kv1.3 (KCNA3) is a rapidly inactivating voltage-gated potassium ion channel of the Shaker family present in many excitable cells. In lymphocytes, plasma membrane-localized Kv1.3 at "immunological synapses" plays a key role in antigen-mediated activation [1]. Furthermore, it is now clear that intracellularly localized Kv1.3 most likely on the inner mitochondrial membrane (mito-Kv1.3) regulates cellular apoptosis. It has been suggested that K^+ cation influx from the intracellular compartment into the mitochondria depolarizes the mitochondrial potential Ψ_{mito}, and hyperpolarization of Ψ_{mito} from blocking mito-Kv1.3 triggers apoptosis [2, 3]. Bax, a pro-apoptotic member of the Bcl-family protein, interacts with mito-Kv1.3 in a residue-specific manner providing a mechanistic hypothesis to Bax-induced apoptosis via blockade of Kv1.3. Consistent with this proposed pro-survival role of mito-Kv1.3, extracellularly applied small molecule membrane-permeable Kv1.3 blockers trigger apoptosis of several different cancer cells richly expressing this ion channel both in vitro and in vivo [4].

Paradoxically, cells devoid of Kv1.3 show resistance to cytotoxic agents [5], suggesting a pro- death role of this ion channel. In conditions such as during sepsis, burn, and other acute injury, pro-apoptotic milieu causes early death of T lymphocyte by both intrinsic and extrinsic pathways and the consequent hypo-immune phase is thought to play a significant pathophysiological role in death from sepsis [6]. The proapoptotic milieu present in sepsis is complex consisting of proapoptotic cytokines, death receptor ligands, proteases, lipid mediators, nitric oxide and mediators resulting from the activation of the compliment and the coagulation systems and the precise death inducing stimuli responsible for lymphocyte apoptosis in sepsis have not been defined. Nevertheless, preventing lymphocyte apoptosis and preventing the consequent immunosuppression has been proposed as a novel approach for the treatment of sepsis (reviewed in [7, 8]).

We wondered whether a selective inhibition of intracellular Kv1.3 might provide relative resistance to cytokine-induced apoptosis mimicking the Kv1.3-null cells. To better understand the consequence of selective inhibition of intracellular Kv1.3, we created a lentivirus designed to intracellularly express the highly selective Kv1.3 blocker peptide agitoxin (AgTX). We created a Jurkat lymphocyte cell line with constitutive intracellular expression of agitoxin and investigated the effects on cytokine-induced apoptosis.

2. Materials and Methods

2.1 Cell culture

Jurkat cells (American Type Culture Collection (ATCC), Manassas, VA, TIB-152) were cultured in RPMI 1640 medium supplemented with 10% heat inactivated fetal calf serum and penicillin/ streptomycin antibiotics. CTLL-2 cells (ATCC, TIB-214) were grown in the same media further supplemented with 10% T-STIM (BD Biosciences, Bedford, MA, #354115). Human embryonic kidney (HEK) 293 cells (ATCC, CRL-1573) were cultured in DMEM (4.5 g/L glucose, 10% fetal calf serum, and penicillin/ streptomycin).

Natural agitoxin consists of 3 different 38 aa peptides agitoxin 1-3 all demonstrating high-affinity inhibition of Kv1.3 [9]. We chose to express agitoxin-2 since this isoform was commercially available as a purified peptide toxin. The Jurkat human T-cell lymphoma cell line was genetically engineered with lentivirus expressing (1) Agitoxin-2 (AgTX) with the sequence: GVPIN VSCTG SPQCI KPCKD AGMRF GKCMN RKCHC TPK and enhanced green fluorescent protein (EGFP), (2) scramble AgTX (same amino acid

composition as the AgTX peptide but with a scrambled sequence): INDVA GRKCN QSPCT KSPGP TCMGP CICMF KRKHK CVG and EGFP, (3) mouse Bcl-2 and EGFP or (4) EGFP alone, and sorted by BD FACS Aria II to isolate the transduced cells with intracellular expression of AgTX, scramble AgTX, Bcl-2 or EGFP alone, respectively. The newly created cell lines were not subjected to clonal selection and all lines are mixture of cells. CTLL-2 cell lines expressing the Kv1.3 constructs (full length or core domain) with co-expression of EGFP were created in a similar manner after transducing the wild-type CTLL-2 cells with lentivirus and cell sorting for EGFP fluorescence.

2.2 Molecular biology

Top and bottom single stranded DNA oligonucleotides encoding the amino acid sequences flanked by restriction enzymes sites, Kozak sequence, start Met, and a stop codon, were synthesized, annealed, and subcloned into the viral vector (Supp Figure 1). Lentivirus was created by a triple transfection of HEK293T cells (ATCC, CRL-11268) with a shuttle vector with the gene of interest subcloned, pVSVG (pMD2.G) for psuedo-typing, and pΔ8.9 (psPAX3) packaging-plasmid (both gifts from Didier Trono). For expression of gene-of-interest, a modified pLL 3.7 shuttle vector (gift from Luk Parijs) where the CMV promoter drives both the expression of the gene and the EGFP reporter was used (see Figure 2). All plasmids were obtained from Addgene (Watertown, MA). The resulting lentivirus expressed the EGFP reporter for easy identification of transduced cells and sorting by a cell sorter for further expansion of a mixture of transduced cell population.

For creation of 3'HA-tagged Kv1.3 inserts, FL or Core-cDNA were amplified from human Kv1.3 clone (NM_002232) using the primers listed in Supplemental Figure 1. The forward primers (Kv1.3-FL-F1 and Kv1.3-Core-F) contained a Kozak sequence followed by the ATG start codon and the reverse primers (Kv1.3-FL-R1 and Kv1.3-Core-R) introduced a Mlu I restriction enzyme site for subcloning into a HA-tagged vector where the tag sequence was inserted between the Mlu I and Not I sites of the pCIneo (Promega, Madison, WI) expression vector. The viral vector technology and molecular manipulations of cDNA to create various tagged constructs were achieved using standard methods. All clones created in house and those obtained from outside vendors were sequenced and the identity and fidelity of the constructs confirmed. RT-PCRs were performed using selective primer pairs targeting agitoxin, scramble agitoxin or EGFP using SuperScript III one-step RT-PCR reagent (Invitrogen, Carlsbad, CA) from 500 ng of total RNA on a RoboCycler thermal cycler (Stratagene, La Jolla, CA).

2.3 Apoptosis assays

Tumor necrosis factor (TNF)-α + cycloheximide (CHX) or Fas ligand (Fas-L) alone were used as the sepsis-mimetic apoptotic agents. These are reasonable sepsis-mimetic pro-apoptotic agents acting on extrinsic, intrinsic, and the endoplasmic reticulum (ER) stress pathways. Preliminary concentration-response studies using caspase 3-like activity as the readout defined the effective concentration ranges for each of the ligands (see Supp Figure 2). TNF-α (100 ng/ ml) + CHX (500 ng/ ml) were applied for 1.5 and Fas-L (1 ng/ ml) for 3 h in a serum-free medium, and where noted, membrane-impermeant recombinant peptide toxin AgTX- 2 (#RTA-150) Alomone Labs, Jerusalem, Israel) or membrane-permeable Kv1.3 blocking molecule 5-(4-phenoxybutoxyl)-psoralen (PAP-1) (P6124, Sigma-Aldrich, St. Louis, MO) were added 30 min prior to ligands application. Standard methods were used for apoptotic read-outs by assessment of DNA

fragmentation, TdT-mediated dUTP nick-end labeling (TUNEL) staining, Western blot for mitochondrial cytochrome C release, and caspase 3-like reporter assay using acyl-Asp-Glu-Val-Asp (Ac-DEVD)-7-amino-4-methylcoumarin (AMC) (Biomol International, Plymouth Meeting, PA).

2.4 Detection of cytokine production and cytokine mRNA expression

Jurkat cells (2 x 10^6/ ml) were plated in 12-well plates in the presence or absence of 10 ng/ ml phorbol-12-myristate-13- acetate plus 0.5 μM ionomycin (PMA + IoM) or 25 μg/ ml concanavalin A (ConA) and incubated for 24 h. The supernatant was collected and IL-2 and TNF-α were measured in triplicates (Quansys Biosciences, West Logan, UT). Total RNA was isolated by Absolutely RNA miniprep kit (Stratagene) and first strand cDNA was synthesized from 500 ng total RNA using RT^2 First Strand kit (SABiosciences, Frederick, MD), then amplified on a Stratagene MX3000p using RT^2 SYBR Green/ Rox qPCR Master Mix kit (SABiosciences). The Rox signal served as an internal standard. The threshold C_T values were determined using the amplification-based threshold detection default mode of the instrument and the data was analyzed using the $2^{-\Delta\Delta C}$T method. Validated primer pairs for IL-2 (#PPH001723), TNF−α (#PPH00341E) and β-actin (#PPH00073E) were obtained from SABiosciences and a preliminary experiment with a 1000- fold dilution of the input cDNA confirmed a linear standard curve and comparable efficiency for both templates using the above primers. All qRT-PCR measurements were performed in triplicates.

2.5 Fluorescence-activated cell sorting (FACS)

After 1.5 h incubation with 1 ng/ ml Fas-L, Jurkat cells were labeled with sulforhodamine 101-conjugated annexin V (Biotium, Hayward, CA) and analyzed for annexin positive apoptotic cells using a BD Biosciences FACS LSRII. Approximately 10,000 cells were counted per sample. Data analysis was performed off-line with the FlowJo software (www.FlowJo.com).

2.6 Western blot analysis

Western blots was performed using standard methods and the sources of the primary antibodies used were: Cytochrome C (1:1000, Abcam, ab133504, Cambridge, MA), Bcl-2 (1:1000, BD Transduction Laboratories, #610538, San Jose, CA) and α-tubulin (1:5000, Abcam, ab7291).

2.7 High performance liquid chromatography (HPLC)

The agitoxin-2 peptide (purchased from Alomone Labs, or present in the cell lysate) was detected by a C18 reverse phase high pressure liquid chromatography equipped with a model L2130 pump and model L2420 UV-Vis detector (Hitachi Instruments, San Jose, CA) set at a wavelength of 215 nm using a linear gradient of isopropyl alcohol/ acetonitrile (2:1) with 0.1% trifluoroacetic acid (27 to 43%) over 40 minutes at a flow rate of 0.3 ml/ min. Absorbance peak at around 19 minutes retention time corresponded to the agitoxin peptide.

2.8 Statistical analysis

Comparison of the means (caspase activity, cytochrome c release, TUNEL positive cell counts, etc.) was by the Mann-Whitney non-parametric test at $P<0.05$ level of significance.

3. Results

3.1 Stable expression of intracellular AgTX

Since no reagents capable of exclusively blocking the intracellular Kv1.3 exist, we created a lentivirus vector to selectively express the Kv1.3-blocking agitoxin

peptide in the cytosol. cDNA encoding the 38 amino acid agitoxin peptide was incorporated into a lentivirus shuttle vector designed to co-express the EGFP reporter following an IRES sequence (Figure 1A). Jurkat cells were transduced with the lentivirus vector and the EGFP fluorescence used to sort the cells (Figure 1B). The near-homogeneous post-sort Jurkat cells (Figure 1C) expressing agitoxin (Jurkat-AgTX), scrambled agitoxin where the same amino acids were expressed in a scrambled order (Jurkat- scramble), Bcl-2 (Jurkat-bcl-2) or EGFP (Jurkat-EGFP) alone were propagated up to 10 passages until used for experiments. A Western blot probed with anti-bcl-2 antibody confirmed the overexpression of the Bcl-2 protein in the Jurkat-bcl-2 line (Figure 1D) and a RT-PCR analysis with sequence specific primers confirmed the presence of the agitoxin or the scrambled mRNA (Figure 1E). We were not able to confirm the presence of the agitoxin or the scrambled proteins in the respective cell lines by immunochemical methods because no antibody was available and our efforts to generate an anti-agitoxin antibody by inoculating rabbits with the traditional KLH- or MAP- 9 [10] conjugated peptide antigen failed. However, a reverse phase HPLC analysis of the Jurkat-AgTX cell lysate revealed a peak at the same retention time as the control agitoxin peptide consistent with a successful expression and folding of this toxin in the cell (Figure 1F).

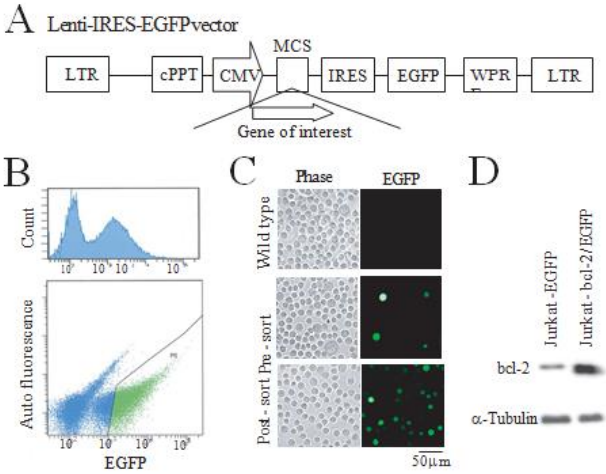

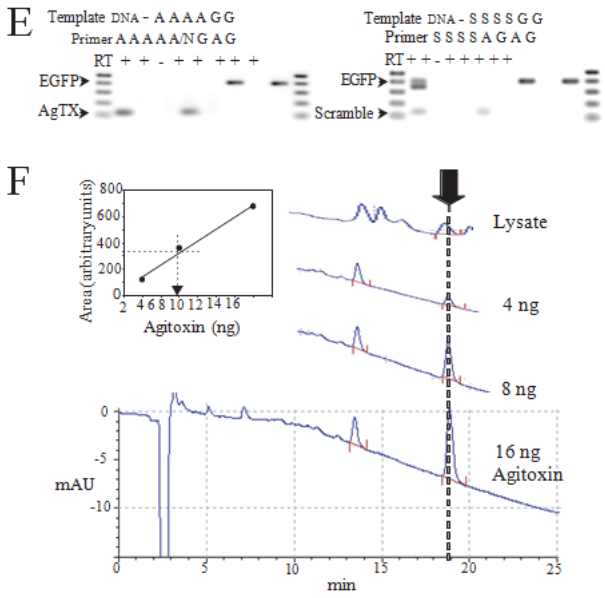

Figure 1: Lentivirus-mediated creation of cell lines. (A) Lentivirus shuttle vector used for the expression of gene-of-interest that allows co-expression of an EGFP reporter. Note that the reporter cDNA is placed after an IRES sequence allowing the expression of separate proteins; (B) A cell-sorter report demonstrating an EGFP peak corresponding to the transduced cells (top) and a typical selection criterion for isolating the transduced cells (bottom, green dots); (C) Phase and fluorescent images of wild type Jurkat cells (top), lentivirus transduced and pre-sort (middle) or post-sort (bottom); (D) A western blot of cell lysates from EGFP expressing Jurkat (Jurkat-EGFP) and bcl-2 expressing Jurkat (Jurkat-bcl-2/EGFP) demonstrating bcl-2 overexpression in the latter cell line. α-tubulin immuno blot served as a protein loading control; (E) A RT-PCR confirmation of the expression of agitoxin (AgTX, left) and scrambled agitoxin (scramble, right) in lentivirus transduced Jurkat cell lines. Template "DNA" is a plasmid viral shuttle vector expressing AgTX (left) or scramble AgTX (right), "A" denotes AgTX expressing Jurkat-AgTX, "G" for Jurkat- EGFP, "S" for scramble-Jurkat. Primer pair "A" is an AgTX , "N" is nonspecific, "G" is EGFP, "S" is scramble AgTX- specific primer

sets. The respective expected products (400 bp for EGFP and 120 bp for AgTX and Scramble) are denoted by arrows. Note the presence of nonspecific products nearly identical in size to the EGFP product amplified by the scramble primer set for the control plasmid template; (F) The agitoxin peptide was detected by an HPLC. Traces are from three amounts of purified agitoxin peptide and a cell lysate from Jurkat-AgTX subjected to the HPLC analysis. The full elution profile is shown for the 16 ng sample trace with only the relevant portions shown for the other runs. The arrow represents the elution peak at around 19 min corresponding to the agitoxin peptide. The inset panel shows a three-point standard calibration for area vs. agitoxin amount with a superimposed linear regression line. The dotted line represents an estimate of the agitoxin amount present in the cell lysate (about 7.5 ng for this sample). The agitoxin peak was absent in a lysate prepared from control Jurkat cells. mAU: arbitrary absorbance units.

3.2 Intracellular expression of AgTX confers relative resistance to apoptosis

We used TNFα plus cycloheximide, or Fas-L alone as our proapoptotic stimuli. First, we demonstrated that these stimuli induced apoptosis of control Jurkat cells as assessed by TUNEL staining, DNA fragmentation, and caspase 3-like activity (Supp Figure 2). Next, we investigated the effects of the cytokines on caspase 3-like activity in the engineered Jurkat lines. Both Fas-L and TNFα plus cycloheximide stimulation resulted in the induction of caspase 3-like activity in all Jurkat lines. Figures 2A1 and 2A2 show the responses after subtraction of the pre-induction baseline activity normalized to the Jurkat-EGFP response. External application of AgTX (100 nM) did not reduce the caspase activity while Jurkat-AgTX and the Jurkat-Bcl-2 lines demonstrated less caspase 3-like activity. Cells expressing the scrambled AgTX did not demonstrate reduction of stimuli-induced activation of the caspase 3-like activity. As expected, an overexpression of Bcl- 2 reduced the cytokine-induced apoptosis. A membrane permeable Kv1.3 inhibitor PAP-1 also reduced the caspase activity at concentrations close to the EC_{50} [11] but this protective effect was lost at higher concentrations (Figure 2B). This loss of inhibition of caspase activity at the higher concentrations could be due to concurrent inhibition of the plasma membrane Kv1.3 or other K-channels since the selectivity of PAP-1 is lost at the higher concentrations blocking other members of the Kv1.x family [12]. In a separate assay, Fas-L-induced mitochondrial release of cytochrome C was likewise reduced in the Jurkat-AgTX line compared to the Jurkat-EGFP cells, with no effect of extracellular AgTX on this measure of apoptosis either (Figure 2C).

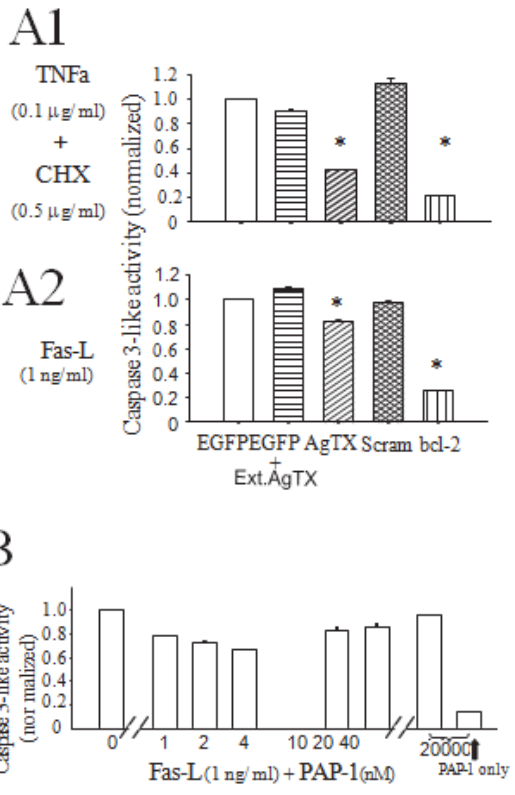

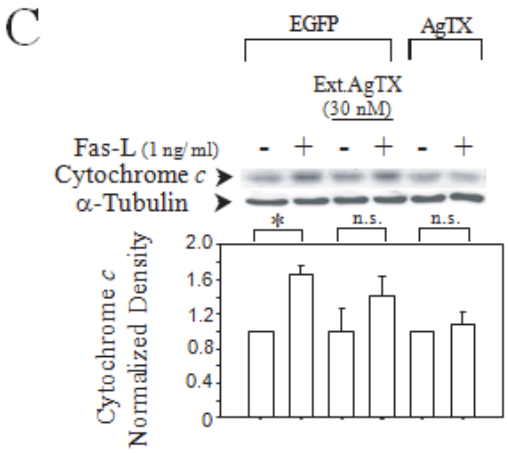

Figure 2: Jurkat-AgTX cells showed relative inhibition of cytokine induction of caspase-3 like activity and mitochondrial release of cytochrome C. (A1) Effects of TNFα (100 ng/ ml) + CHX (500 ng/ ml); (A2) Fas-L (1 ng/ ml) on caspase 3-like activity in four different engineered Jurkat cell lines: wild type (control with only EGFP expression, blank bar), AgTX (agitoxin/ EGFP, diagonal lines), Scramble (scramble agitoxin/ EGFP, crossed lines), bcl-2 (bcl-2/ EGFP, vertical lines). The bars with horizontal lines are for EGFP control cells with the addition of 30 nM extracellular agitoxin. Data (mean ± S.E.M.) from triplicate measurements. The experiment was performed three times with similar results. * P<0.05; (B) Effects of PAP-1 on Fas-L (1 ng/ ml) induced caspase 3-like activity. PAP-1 reduced the activity at concentrations close to Ec50 for Kv1.3 (2 ± 0.2 nM). High concentration of PAP-1 itself didn't induce caspase 3-like activity (far right bar); (C) A Western blot detection of cytochrome *c* release from the mitochondria by Fas-L. Wild type EGFP Jurkat-control or Jurkat-AgTX cells were incubated in Fas-L (1 ng/ ml) for 1.5 hrs with or without external application of 30 nM agitoxin. The cytosolic protein was extracted by freeze-thaw cycles and the extract subjected to a Western blot analysis (top). α-tubulin normalized cytosolic cytochrome c densitometry (bottom). Data are mean ± S.E.M. from four independent experiments.

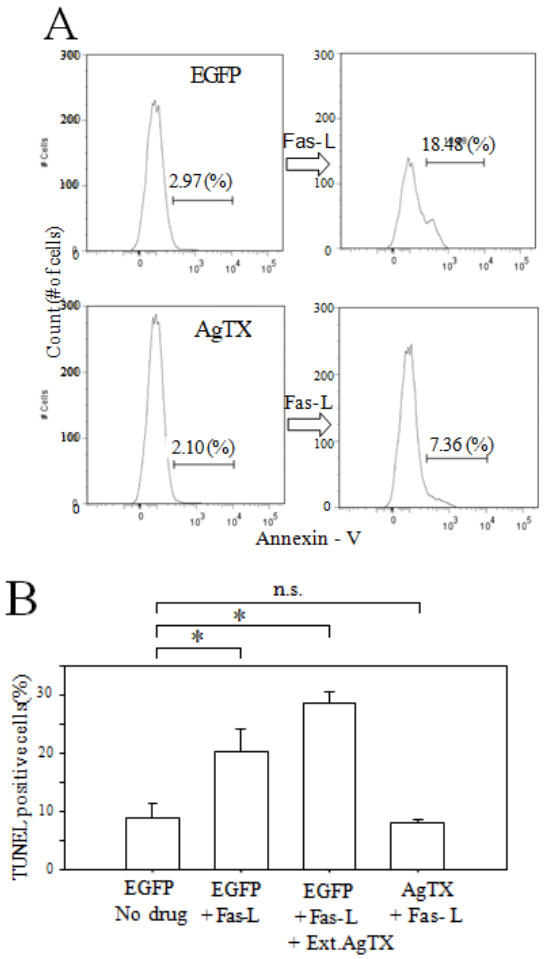

Figure 3: Jurkat-AgTX cells demonstrated relative resistance to Fas-L induced apoptosis. (A) Analysis of annexin V positive apoptotic cells by flow cytometry. Wild type EGFP Jurkat- control or Jurkat-AgTX cells were incubated in Fas-L (1ng/ml) containing culture media for 1.5 hrs and labeled with sulforhodamine-conjugated annexin V. After Fas-L stimulation, about 18.5% cells were annexin V positive in control but the number was reduced to about 7% for Jurkat-AgTX; (B) A histogram summary of TUNEL positive cells (mean ± S.E.M. from triplicate counts) after 3 hrs Fas-L stimulation. External application of agitoxin did not reduce the number of TUNEL positive cells. *P<0.05.

Further assessments of the relative apoptosis resistance of the Jurkat-AgTX compared to the control Jurkat-EGFP cells were done by a flow cytometer assay of

annexin-V positive cell count (Figure 3A) and a manual TUNEL positive cell count (Figure 3B) after Fas-L stimulation. We again confirmed that the cells engineered to express AgTX in the cytosol exhibited relative resistance to apoptosis.

3.3 Engineered cells show normal production of IL-2 and TNF-a

Activation of T-lymphocytes upon antigen presentation resulting in the induction of cytokine production constitutes the normal initial response. We wanted to confirm that this critical normal initial response to activation was preserved in the Jurkat-AgTX cells since our goal was to design relatively apoptosis-resistant T-lymphocytes able to survive the apoptotic milieu such as those present during sepsis, yet capable of mediating the host defense response presumably necessary to enhance survival in sepsis. Jurkat-EGFP or –AgTX cells were stimulated with the lecithin ConA or the phorbol ester PMA plus ionomycin; stimuli previously demonstrated to induce proinflammatory cytokine production in Jurkat cells [12]. Both stimuli induced IL-2 and TNF-α transcription, as assessed by qRT-PCR analysis of the cells (Supp Figure 3), and secretion, as assessed by ELISA analysis of the culture media, confirming that the overexpression of AgTX did not preclude the normal response of the Jurkat cells to activation.

3.4 Expression of truncated Kv1.3 fails to provide cytoprotection

While ion permeation through the mito-Kv1.3 in the regulation of apoptosis is well supported by abundant literature, there are unresolved issues from a biophysical perspective. Mitochondria exhibit a large negative Ψ_m membrane potential with respect to the cytosol and if the biophysical properties of the mito-Kv1.3 resemble that plasma membrane Kv1.3, channels inserted in the inner mitochondrial membrane sensing a large negative transmembrane potential would be largely closed. Even if the channel were to transiently open, the inactivating Kv1.3 channels would not be open constitutively. This incongruence is yet to be resolved, however, the mito-Kv1.3 appears to be constitutively open since blocking this channel results in hyperpolarization of Ψ_m [13]. We wondered whether sensitization of cells to cytokines would be recapitulated if only the core domain Kv1.3 (Figure 4A) capable of forming an ion permeable channel but devoid of the remainder of the large N- and C-cytosolic domains of the channel protein was reintroduced into a Kv1.3-null cell.

Lentivirus expressing the full length (FL)-Kv1.3 or core domain (Core)-Kv1.3 and EGFP were created, and Kv1.3 null CTLL-2 cell lines constitutively expressing the respective constructs established as before. RT-PCR with insert-specific primers confirmed the presence of the expected FL-Kv1.3 or Core-Kv1.3 in the cells (Figure 4B). It is expected that the Core-Kv1.3 channel is a non-inactivating current since the pore-block type rapid inactivation of the Shaker- type ion channel is mediated by the N-terminal domain residues [14]. Cells were stimulated with the TNF-α and cycloheximide combination, and caspase 3-like activity assayed (Figure 4C). CTLL cells only expressing EGFP showed relative resistance to cytokine stimulation maintaining the Kv1.3-null phenotype, whereas, introduction of FL-Kv1.3 sensitized the cells with increasing caspase 3-like activity consistent with a previous report [5]. In contrast, Core-Kv1.3 expressing cells were not sensitizing demonstrating a phenotype indistinguishable with Kv1.3-null cells.

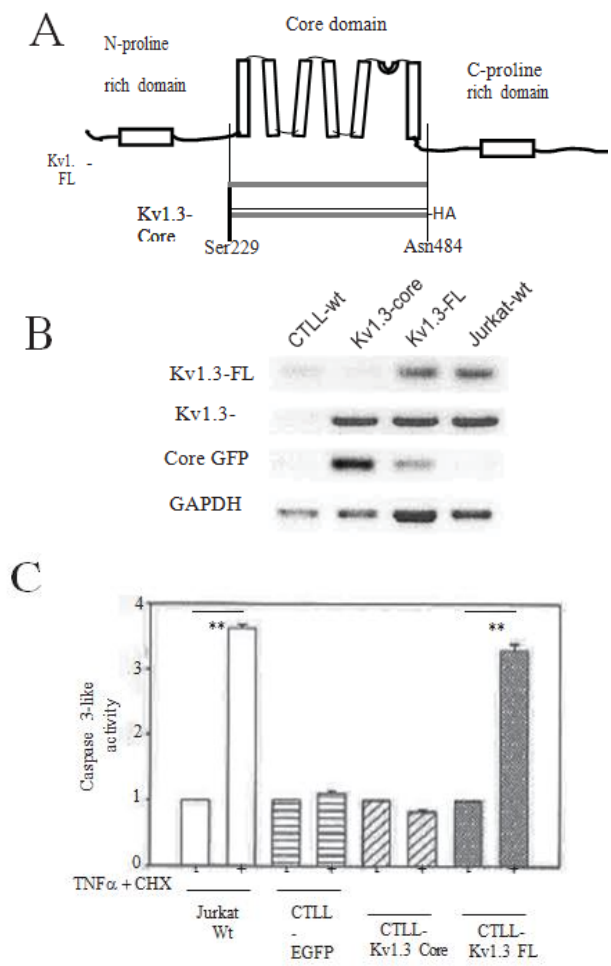

Figure 4: Expression of Kv1.3-Core does not sensitize the CTLL cells to apoptosis. (A) A cartoon (not to scale) of the Kv1.3 channel illustrating the ion conducting transmembrane core domain and the large cytosolic N- and C-terminal domains; (B) Agarose gel electrophoresis of RT-PCR products from the cells as indicated on the top. The primer pairs (see Supp Figure 1) were designed for specific amplification of the products indicated on the left. Kv1.3-FL primers (Kv1.3-FL-F2 and -R2) targeted the region of cDNA outside of the Kv1.3-Core thus only amplified the desired FL cDNA while the Kv1.3-Core primers (Kv1.3-Core-F and -R) amplified both the FL and Core cDNA; (C) Bar plots of Caspase 3-like activity normalized to the Jurkat-wt cells with no stimulation. Cells were stimulated with TNF-α + CHX as specified in Methods. Data are mean ± S.E.M. from three independent experiments. **P<0.001. Results for CTLL- EGFP and CTLL-Kv1.3-Core for – and + stimulus were not significantly different at P>0.05.

4. Discussion

Cytosolic expression of the selective Kv1.3 blocker AgTX conferred relative resistance to apoptosis induced by TNFα or Fas-L stimulation. This cytoprotective effect was not mimicked by extracellular application of AgTX supporting the specific role of inhibition of intracellular Kv1.3. Cells constitutively expressing intracellular AgTX behaved similar to Kv1.3-deficient cells previously shown to be resistant to multiple apoptosis inducers initially reported by Bock et al. [5] and subsequently confirmed by several reports [2-4]. The invariant HPLC retention time of intracellularly expressed AgTX from control biologically active AgTX strongly suggests proper folding of the expressed toxin even within the relatively reduced intracellular environment. However, we acknowledge that the assumption that the intracellularly expressed AgTX was properly folded and biologically active has not been shown directly.

The seemingly contradictory observation that cells lacking Kv1.3 show resistance to cytokine- induced apoptosis, while inhibition of mito-Kv1.3 by plasma membrane permeable small- molecules kill cells, was specifically noted in an earlier study [2] where the authors stated, “deficiency of Kv1.3 is clearly not equivalent to inhibition of the channel.” The absence of chronic Ψ_m depolarization due to mito-Kv1.3 in cells lacking this ion channel and difference in the basal cellular ROS level in normal vs. cancer cells have been pointed out as potential reasons for the differential sensitivity of various cells to membrane permeable small molecule Kv1.3 inhibitors. Past studies, while

yielding convincing results, shared the fundamental limitation that the genetic and pharmacological models employed, to some degree, inhibit both plasma membrane and mito- Kv1.3 channels. Kv1.3-null cells lacked both plasma membrane and mito-Kv1.3 and gain of function studies by Kv1.3 transfection re-introduced both plasma membrane and mito-Kv1.3. An exception to this was the apparent resensitization of Kv1.3-null cells to drug-induced apoptosis after transfection-mediated intracellular expression of a mitochondrially-targeting Kv1.3 [13]. Pharmacological studies comparing small molecule membrane-impermeant (e.g. AgTX and margitoxin) and -permeant (e.g. Psora-4, Pap-1, and clofazimine) inhibitors blocked the plasma membrane or both Kv1.3 channels, respectively, and did not provide definitive conclusion on the consequences of only inhibiting mito-Kv1.3. Due to the high selectivity of AgTX for Kv1.3 [15], we believe our current study is the first to report on the consequence of only inhibiting intracellular Kv1.3. A more recent effort at developing extracellularly applied targeting pro-drugs incorporating lipophilic cations could enable a more efficient targeting of intracellular organelles, including the mitochondria [16]. Our cellular assays (caspase-3 activity, cytochrome-C release, DNA fragmentation, TUNEL staining) focused on apoptosis consistent with signaling initiated in the mitochondria but Kv1.3 has a broad intracellular expression [17] and expression of intracellular AgTX, in theory, could block Kv1.3 activity in all intracellular organelles. Therefore, our study was unable to specify mito-Kv.3 as the site conferring relative resistance to cytokine-induced cell death.

Our observation that the introduction of a truncated ion channel-forming Core-Kv1.3 into the Kv1.3-null CTLL cells did not sensitize the cells to cytokine-induced apoptosis is intriguing. In addition to the currently accepted view that apoptosis regulation by Kv1.3 is mediated through ion permeation, could apoptosis regulation be mediated by the non-ion permeating segments of the channel protein? Ion channels conduct ions; however, they are complex proteins with well-defined protein interaction motifs as well. The Kv1.3 channel possesses both N- and C-terminal proline- rich motifs likely recognized by src-homology (SH)-3 domain containing signaling molecules [18] and this protein motif is essential for the guanylate kinase modulation of the ion channel function. Our data indicating that the truncated Kv1.3 core ion channel devoid of the N- and C-terminals but capable of forming a non-inactivating functional ion pore does not sensitize the CTLL-2 mouse lymphocyte to apoptosis suggests a critical role of the non-ion permeating protein domain in the regulation of apoptosis. Confirming the intriguing possibility that the non-plasma membrane Kv1.3 may regulate apoptosis through protein: protein interactions rather than through ion permeation will require further studies.

In sepsis, increased leukocyte apoptosis occurred in CD4+ and CD8+ T lymphocytes, CD20+ B lymphocytes, and CD56+ natural killer cells are seen in blood samples. Activated caspases 8 and 9 were seen in apoptotic T lymphocytes, suggesting that both the death receptor-mediated extrinsic pathway and the mitochondria-mediated intrinsic pathways played a role [6]. Conferring relative resistance to lymphocytes to survive the pro-apoptotic milieu of early sepsis by selectively inhibiting mito-Kv1.3, while preserving lymphocyte activation where plasma membrane Kv1.3 plays a critical role, may enable a novel adoptive transfer therapy of engineered-T lymphocytes for sepsis expanding the role of Kv1.3 as a therapeutic target for various pathologies [19].

5. Conclusion

This study demonstrated that intracellular expression of the highly selective Kv1.3 peptide inhibitor in Jurkat lymphocytes conferred relative resistance to cell death induced by pro- apoptotic cytokines. Such a virus-mediated selective inhibition of intracellular Kv1.3 could be a new therapeutic strategy to fight sepsis and other pathologies where early lymphocyte apoptosis plays a critical role in diseases progression.

Acknowledgements

This research was partly supported by NIH RO1 GM071485, GM086401, and the Bamforth Endowment funds from the Department of Anesthesiology, University of Wisconsin SMPH (JY) and Japan Society for the Promotion of Science (KAKEN) 17K11592 (TS).

Conflict of Interest

The authors declare that they have no competing interests.

References

1. Panyi G, Varga Z, Gaspar R. Ion channels and lymphocyte activation. Immunol Lett 92 (2004): 55-66.
2. Szabo I, Bock J, Grassme H, et al. Mitochondrial potassium channel Kv1.3 mediates Bax-induced apoptosis in lymphocytes. Proc Natl Acad Sci USA 105 (2008): 14861-14866.
3. Szabo I, Soddemann M, Laenza L, et al. Single-point mutations of a lysine residue change function of Bax and Bcl-Xl expressed in Bax- and Bak-less mouse embryonic fibroblasts: novel insights into the molecular mechanisms of Bax-induced apoptosis. Cell Death Differentiation 18 (2011): 427-438.
4. Laenza L, Henry B, Sassi N, et al. Inhibitors of mitochondrial Kv1.3 channels induce Bax/Bak-independent death of cancer cells. EMBO Mol Med 4 (2012): 577-593.
5. Bock J, Szabo I, Jekle A, et al. Actinomycin D-induced apoptosis involves the potassium channel Kv1.3. Biochem Biophys Res Commun 295 (2002) 526-531.
6. Hotchkiss RS, Osmon SB, Chang KC, et al. Accelerated lymphocyte death in sepsis occurs by both the death receptor and mitochondrial pathways. J Immunol 174 (2005): 5110-5118.
7. Hotchkiss RS, Monneret G, Payen D. Sepsis-induced immunosuppression: from cellular dysfunctions to immunotherapy. Nat Rev Immunol 13 (2013): 862-874.
8. Girardot T, Rimmelé T, Venet F, et al. Apoptosis-induced lymphopenia in sepsis and other severe injuries. Apoptosis 22 (2017): 295-305.
9. Garcia ML, Garcia-Calvo M, Hidalgo P, et al. Purification and characterization of three inhibitors of voltage-dependent K channels from Leiurus quinquestriatus var. herbraeus venom. Biochemistry 33 (1994): 6834-6839.
10. Posnet DN, McGrath H, Tam JP. A novel method for producing anti-peptide antibodies. J Biol Chem 263 (1988): 1719-1725.
11. Schmitz A, Sankaranarayanan A, Azam P, et al. Design of PAP-1, a selective small molecule Kv1.3 blocker, for the suppression of effector memory T cells in autoimmune diseases. Mol Pharmacol 68 (2005): 1254-1270.
12. Slifka MK, Whitton JL. Antigen-specific regulation of T cell-mediated cytokine production. Immunity 12 (2000): 451-457.
13. Szabo I, Bock J, Jekle A, et al. A novel potassium channel in lymphocyte

mitochondria. J Biol Chem 280 (2005): 12790-12798.

14. Hoshi T, Zagotta WN, Aldrich RW. Biophysical and molecular mechanisms of Shaker potassium channel inactivation. Science 250 (1990): 533-538.
15. Szabò I, Leanza L. The roles of mitochondrial cation channels under physiological conditions and in cancer. Handb Exp Pharmacol 240 (2017): 47-69.
16. Mattarei A, Romio M, Managa A, et al. Novel mitochondria-targeted furocoumarin derivatives as possible anti-cancer agents. Font Oncology 8 (2018): 1-8.
17. Leanza L, Biasutto L, Managò A, et al. Intracellular ion channels and cancer. Front Physiol 4 (2013): 1-7.
18. Marks DR, Fadool DA. Post-synaptic density perturbs insulin-induced Kv1.3 channel modulation via a clustering mechanism involving the SH3 domain. J Neurochem 103 (2007): 1608-1627.
19. Perez-Verdaguer M, Capera J, Serrano-Novillo C, et al. The voltage-gated potassium channel Kv1.3 is a promising multitherapeutic target against human pathologies. Exp Opin Ther Targets 20 (2016): 577-591.